Journal of Medicinal Chemistry

Article

Cite This: J. Med. Chem. XXXX, XXX, XXX−XXX

pubs.acs.org/jmc

Discovery and Optimization of Selective and in Vivo Active Inhibitors of the Lysophosphatidylserine Lipase α/β-Hydrolase Domain-Containing 12 (ABHD12)

Daisuke Ogasawara,*,† Taka-Aki Ichu,† Hui Jing,† Jonathan J. Hulce,† Alex Reed,‡ Olesya A. Ulanovskaya,‡ and Benjamin F. Cravatt*,†

†Department of Chemistry, The Scripps Research Institute, 10550 N. Torrey Pines Road, La Jolla, California 92037, United States

‡Abide Therapeutics, 10835 Road to the Cure, San Diego, California 92121, United States

Supporting Information

ABSTRACT: ABHD12 is a membrane-bound hydrolytic enzyme that acts on the lysophosphatidylserine (lyso-PS) and lysophosphatidylinositol (lyso-PI) classes of immunomodulatory lipids. Human and mouse genetic studies point to a key role for the ABHD12-(lyso)-PS/PI pathway in regulating (neuro)immunological functions in both the central nervous system and periphery. Selective inhibitors of ABHD12 would offer valuable pharmacological probes to complement genetic models of ABHD12-regulated (lyso)-PS/PI metabolism and signaling. Here, we provide a detailed description of the discovery and activity-based protein profiling (ABPP) guided optimization of reversible thiourea inhibitors of ABHD12 that culminated in the identification of DO264 as a potent, selective, and in vivo active ABHD12 inhibitor. We also show that DO264, but not a structurally related inactive control probe (S)-DO271, augments inflammatory cytokine production from human THP-1 macrophage cells. The in vitro and in vivo properties of DO264 designate this compound as a suitable chemical probe for studying the biological functions of ABHD12-(lyso)-PS/PI pathways.

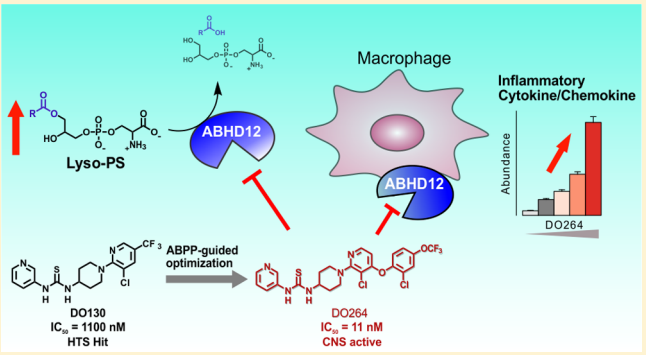

INTRODUCTION

Lysophospholipids represent an important class of signaling lipids that impact diverse physiological and disease processes.[1,2] Prominent lysophospholipid transmitters include lysophosphatidic acid (lyso-PA)[3] and sphingosine 1-phosphate (S1P).[4] These bioactive lipids have cognate receptors, mostly from the G-protein-coupled receptor (GPCR) category, and small-molecule modulators of these receptors have been clinically advanced to treat, for instance, immunological disorders.[4] The magnitude and duration of lysophospholipid action are controlled by specific sets of biosynthetic and degradative enzymes,[5,6] and these enzymes offer additional targets for pharmacological control over lysophospholipid pathways.

In recent years, other bioactive lysophospholipids, such as lysophosphatidylserine (lyso-PS) and lysophoshatidylinositol (lyso-PI), have emerged as signaling molecules that act on distinct subsets of GPCRs,[7−9] as well as possibly other receptor types.[10] Our current understanding of the physiological functions of lyso-PS and lyso-PI is limited and would benefit from selective chemical probes to perturb these lipid pathways in vivo. This challenge can be addressed, in part, by developing synthetic agonists and antagonists of the lyso-PS/PI receptors.[11−13] As noted above, however, an attractive and complementary strategy would be to create inhibitors of the enzymes that produce or inactivate lyso-PS/PI.

In the course of attempting to understand the biochemical basis for rare, monogenic disorders of the central nervous system (CNS) caused by deleterious mutations in enzymes from the serine hydrolase family, we discovered that ABHD12 (α/β-hydrolase domain-containing 12), loss-of-function mutations which cause the neurological disease PHARC (polyneuropathy, hearing loss, ataxia, retinitis pigmentosa, and cataract; MIM 612674),[14,15] is a principal lyso-PS/PI lipase in mammals. Mice with targeted disruption of the *Abhd12* gene show elevated lyso-PS/PI, as well as increased polyunsaturated (C20:4) PS, content in the CNS.[16] These mice also display a subset of PHARC-like abnormalities, including auditory and motor control deficiencies, which emerge later in life (∼10−18 months) and are accompanied by brain microgliosis,[16] suggesting that PHARC may have an immunological underpinning. Also consistent with this premise, ABHD12 is highly expressed in innate immune cells (macrophages, microglia) and several lyso-PS receptors show restricted expression to the immune system.[17,18]

Received: December 13, 2018

DOI: 10.1021/acs.jmedchem.8b01958
J. Med. Chem. XXXX, XXX, XXX−XXX

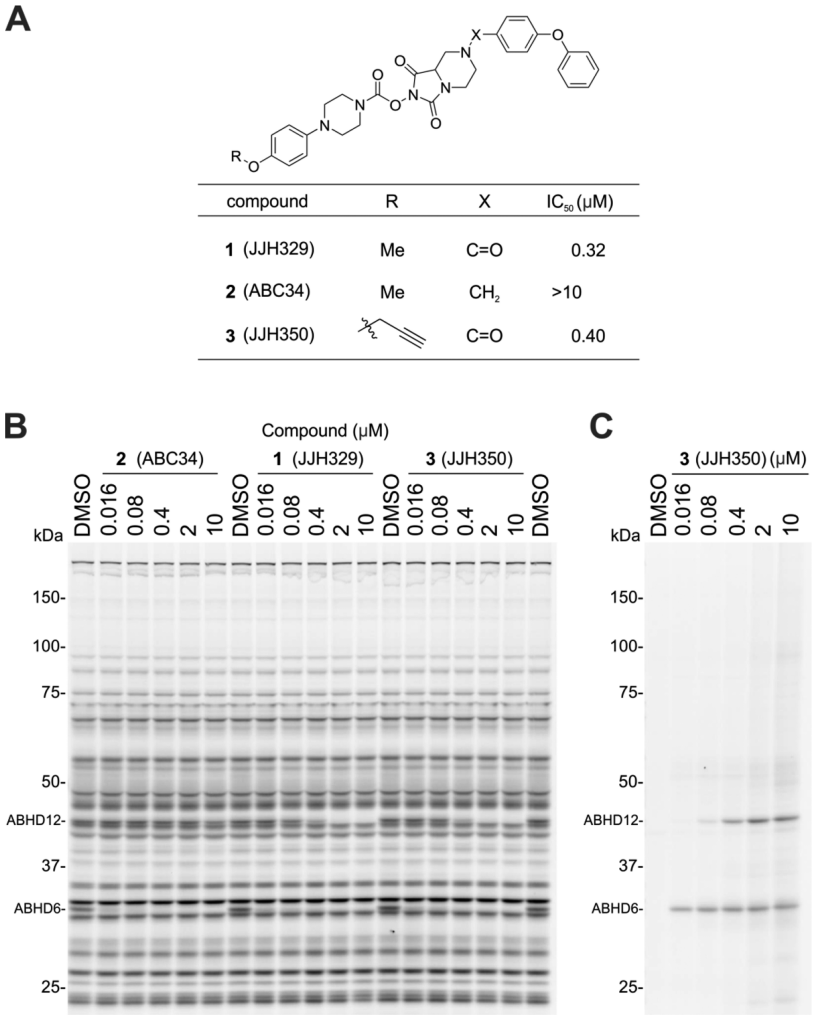

Figure 1. Discovery of NHH-carbamate inhibitors and tailored activity-based probes for ABHD12. (A) Chemical structures and ABHD12 inhibitory activities for the indicated NHH-carbamate compounds. IC_{50} values were determined by gel-based competitive ABPP using the FP-Rh probe. (B) In vitro potency and selectivity of NHH-carbamate compounds in mouse brain membrane proteome as measured by gel-based competitive ABPP using the FP-Rh probe. (C) Visualization of ABHD12 in mouse brain membrane proteome using the JJH350 probe. For the gel-based ABPP assays, mouse brain membrane proteomes (1 mg/mL) were preincubated with NHH-carbamate compounds (45 min, 37 °C) followed by the reaction with FP-Rh probe (1 μM, 45 min, 37 °C) (A, B) or with Rh-N_3 (25 μM) using CuAAC conditions (60 min, rt) (C).

To better understand the contributions of the ABHD12-(lyso)-PS/PI pathway to neuroimmunological processes, we recently reported the discovery of a selective and in vivo active inhibitor of ABHD12.[19] This compound termed DO264, an *N*-3-pyridyl-*N*′-4-piperidinylthiourea, appears to act as a reversible, competitive inhibitor of ABHD12 while showing negligible interactions with other serine hydrolases as determined by activity-based protein profiling (ABPP).[19] We found that DO264-treated mice displayed elevations in brain lyso-PS/PI and C20:4 PS lipids but did not exhibit the auditory defects observed in ABHD12−/− mice, even following 4 weeks of inhibitor treatment. On the other hand, both DO264-treated and ABHD12−/− mice exhibited heightened immunological responses to lymphocytic choriomeningitis virus (LCMV) clone 13 infection in mice, supporting an immunomodulatory function for the ABHD12-(lyso)-PS/PI pathway.

Here, we provide a detailed account of the identification, synthesis, and structure−activity relationship (SAR) of *N*-3-pyridyl-*N*′-4-piperidinylthiourea inhibitors of ABHD12 that led to the discovery of DO264, as well as a structurally related inactive control probe (S)-DO271. We also describe the development of a tailored activity-based probe for ABHD12 (the *N*-hydroxyhydantoin (NHH)-carbamate JJH350) that serves as a versatile target engagement tool for monitoring ABHD12 activity and inhibition in vivo.

RESULTS

Exploration of NHH-carbamates Furnishes JJH350 as a Tailored Activity-Based Probe for ABHD12. We previously described a chemical proteomic assessment of NHH-carbamates as irreversible inhibitors of serine hydrolases.[20] A subset of these compounds showed reactivity toward ABHD12 (e.g, JJH329 (**1**), IC_{50} = 0.32 μM, 95% CI = 0.24−0.41 μM), with a notable dependency on a key amide linker (X, Figure 1A) appended to the NHH piperazine leaving group, without which compounds displayed negligible ABHD12 activity up to 10 μM (e.g., ABC34 (**2**); Figure 1A). JJH329 also showed good selectivity as assessed in mouse brain proteome by gel-based ABPP[21,22] using the broad-spectrum serine hydrolase-directed probe fluorophosphonate-rhodamine (FP-Rh),[23] where ABHD6 was observed as the only off-target (Figure 1B). While ABHD12 activity can be monitored by gel-based ABPP using FP-Rh in mouse brain, we

DOI: 10.1021/acs.jmedchem.8b01958
J. Med. Chem. XXXX, XXX, XXX−XXX

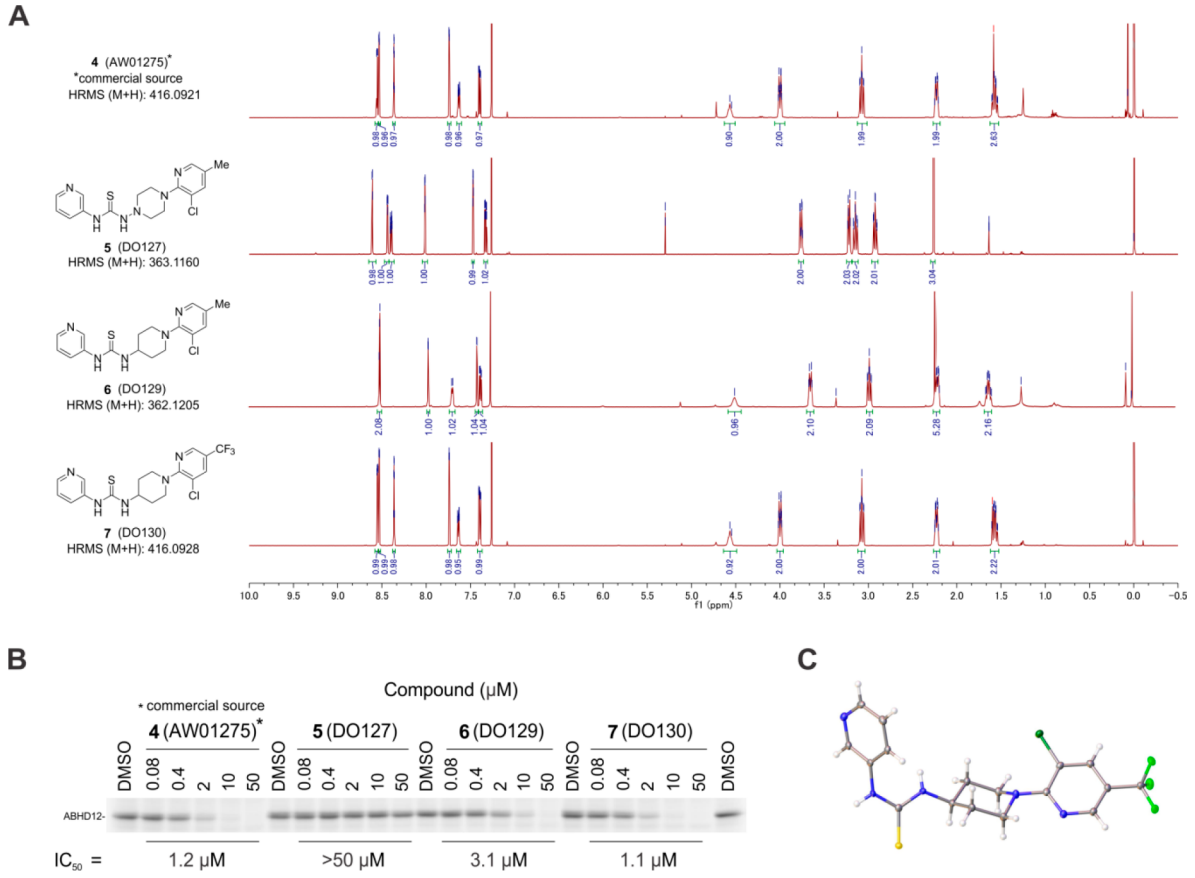

Figure 2. Identification and structure assignment of HTS hit AW01275 as thiourea DO130. (A) Originally assigned chemical structure and ^{1}H NMR of AW01275 (DO127) and its structurally related analogues, DO129 and DO130. The ^{1}H NMR spectra were measured in $CDCl_3$ with D_2O. (B) ABHD12 inhibitory activity of AW01275 (obtained from a commercial source), DO127, DO129, and DO130 as measured by gel-based ABPP of mouse brain membrane proteome (1 mg/mL protein) using the JJH350 probe (2 μM, 45 min, 37 °C). (C) X-ray crystal structure of AW01275 obtained from a commercial source.

found that detection of this enzyme was challenging in other mouse tissues due to overlapping signals from comigrating serine hydrolases.[19] We therefore appended an alkyne handle to JJH329 to furnish an ABHD12-directed activity-based probe JJH350 (**3**) (Figure 1A,B; IC_{50} = 0.40 μM, 95% CI = 0.25−0.62 μM) which enabled direct visualization of ABHD12 by gel-based ABPP following conjugation to an azide-rhodamine reporter group[24] using copper-catalyzed azide−alkyne cycloaddition (CuAAC), or click, chemistry[25] (Figure 1C). ABHD12 (as well as ABHD6) could be clearly visualized in mouse brain proteome across a concentration of 0.4−10 μM of JJH350 (Figure 1C). We then used JJH350 as a target engagement probe to assess the in vivo activity of JJH329, which revealed that JJH329 (30 mg/kg, ip) produced only marginal inhibition of ABHD12 in mice (Figure S1 in Supporting Information). Additional optimization efforts did not lead to the identification of NHH-carbamates that showed better potency in vivo (data not shown). We therefore focused on identifying a new chemotype for ABHD12 inhibitors.

Identification of a Thiourea Class of ABHD12 Inhibitors by Structural Reassignment of the Screening Hit AW01275. We pursued new chemotypes for ABHD12 inhibition by high-throughput screening (HTS) using a fluorescent-coupled substrate assay,[19] and from the Maybridge HitFinder library containing ~16 000 compounds, we identified a putative hit, the thiosemicarbizide AW01275 (**4**, Figure 2A).[19] This compound also inhibited lyso-PS hydrolysis activity of ABHD12 with an IC_{50} value of 1.3 μM[19] and blocked the labeling of ABHD12 by JJH350 with an IC_{50} value of 1.2 μM (95% CI = 0.96−1.4 μM) (Figure 2B). Surprisingly, however, our chemically resynthesized stock of AW01275, termed DO127 (**5**) (Figure 2A), did not show any ABHD12 inhibitory activity as measured with a lyso-PS substrate assay (Figure S2) or by gel-based ABPP (Figure 2B). We found that the ^{1}H NMR and ESI-HRMS of commercial AW01275 did not match the analytical data for DO127 (Figure 2A). In the course of exploring candidate alternative structures, we discovered that a thiourea analogue DO129 (**6**) (Figure 2A) exhibited ABHD12 inhibitory activity (Figure 2B) and peaks in the aliphatic region of the ^{1}H NMR that were similar to those of commercial AW01275 (Figure 2A). We furthermore noted that the ^{13}C NMR spectrum for commercial AW01275 showed a distinct quadruplet (coupling constant of 270.0 Hz) peak indicative of the presence of a CF_3 group (Figure S3). On the basis of these observations, we speculated that the correct structure of AW01275 was the thiourea DO130 (**7**) (Figure 2A), which we subsequently found to display identical ^{1}H NMR, HRMS, and ABHD12 inhibitory activity as commercial AW01275 (Figure 2A,B). X-ray crystallographic analysis of commercial AW01275 confirmed its structural identity as DO130 (Figure 2C). Notably, unlike the irreversible inhibitor JJH350, DO130 did not show time-dependent inhibition of ABHD12 (Figure 3), indicating that this compound and related thioureas act as reversible inhibitors of ABHD12.[19]

DOI: 10.1021/acs.jmedchem.8b01958
J. Med. Chem. XXXX, XXX, XXX−XXX

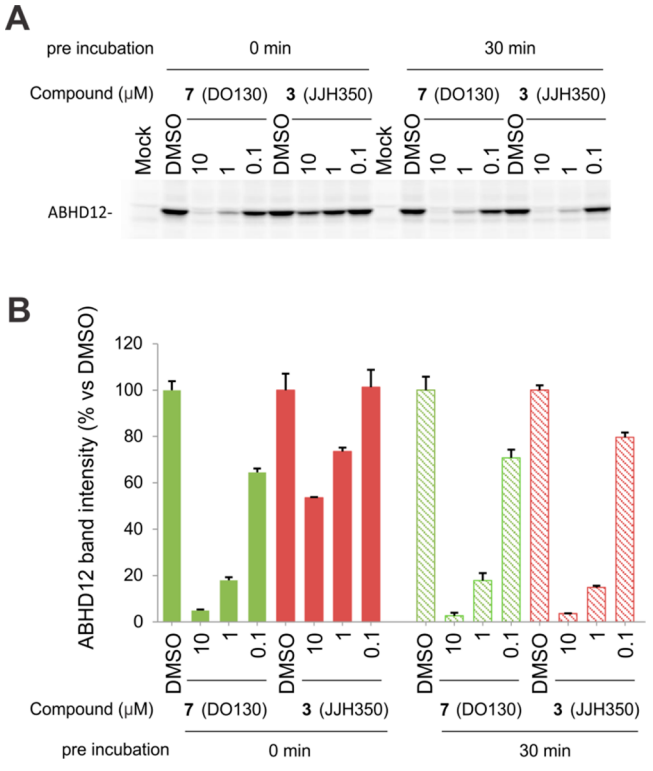

Figure 3. DO130 (**7**) does not show time-dependent inhibition of ABHD12. (A) Comparison of ABHD12 inhibitory activities of JJH350 (**3**) and DO130 (**7**) as measured by gel-based ABPP with membrane lysate of ABHD12-transfected HEK293T cells using an FP-Rh probe (1 μM, 45 min, 37 °C). A representative gel is shown. (B) Bar graph representation of ABHD12 band intensity obtained in (A). $N = 3$. The data represent the mean ± SD.

SAR Analysis of the *N*-Pyridyl Thiourea and Piperidine Core of ABHD12 Inhibitors. We next set out to optimize DO130 and gain a deeper understanding of structural features that contribute to ABHD12 inhibitory activity. These initial investigations of SAR are summarized in Table 1. Given possible concerns of thioureas as potential toxicophores,[26] we first replaced this group with a urea (**8**), but this change resulted in a substantial loss in activity. Next, we explored analogues of the 3-aminopyridine group (R^1), finding that methoxy substitution (**9**) and conversion to 3-aminoquinoline (**10**) or 1,2,3,4-tetrahydroquinoline (**11**) also resulted in diminished potency toward ABHD12 (Table 1A). The phenyl analogue **12** retained some ABHD12 inhibitory activity, albeit slightly lower than that of DO130.

We next focused our attention on the SAR of the piperidine ring system (Table 1B). Repositioning the exocyclic amino group of DO130 to the 3-position (**13**) abolished ABHD12 inhibitory activity, while replacing the piperidine with smaller (5-membered (**14**)) or larger (7-membered (**15**)) ring systems resulted in near-complete loss (**14**) or substantial reductions (**15**) in potency. Acyclic analogues (**16**–**19**) with varying linker lengths (C3–C6) were also tested, and while several displayed modest activity, none were as potent as DO130. *N*-Methyl substitution of the exocyclic amino group (**20**) also weakened ABHD12 activity. Finally, we replaced the piperidine core with 8-azabiocyclo[3.2.1]octane (**21**) to test if conformational constraint might promote ABHD12 inhibition. Like all other deviations from the piperidine system, this too impaired ABHD12 activity relative to DO130. Together, these results demonstrated the importance of the 3-pyridylthiourea and 4-aminopiperidine moieties found in DO130 for ABHD12 activity and suggested a low tolerance to modification in these regions.

Exploration of Pyridine Substituent Effects. In pursuit of ABHD12 inhibitors with enhanced potency, we next explored structure–activity relationships of the distal pyridine group

Table 1. ABHD12 Inhibitor SAR of the *N*-Pyridylthiourea and Piperidine Core

A

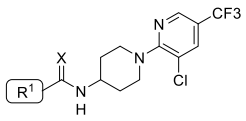

compound	R^1	X	% inhibition 2 μM	% inhibition 10 μM
7 (DO130)		S	89	96
8	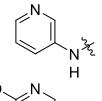	O	1	29
9	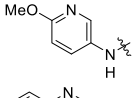	S	0	1
10	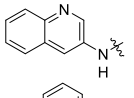	S	0	2
11		S	0	0
12	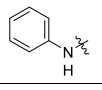	S	66	96

B

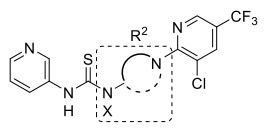

compound	R^2	% inhibition 2 μM	% inhibition 10 μM	compound	R^2	% inhibition 2 μM	% inhibition 10 μM
7 (DO130)	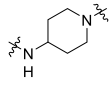	89	96	**17**	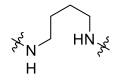	12	35
13	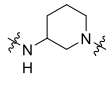	0	4	**18**	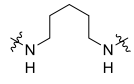	54	90
14	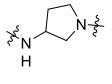	1	12	**19**	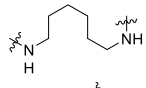	22	70
15	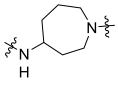	9	59	**20**	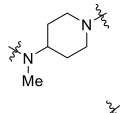	31	61
16	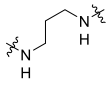	0	0	**21**	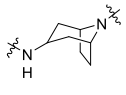	19	63

DOI: 10.1021/acs.jmedchem.8b01958
J. Med. Chem. XXXX, XXX, XXX–XXX

Table 2. Pyridine Substituent Effects on ABHD12 Activity

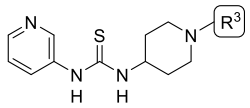

compound	R^3	IC_{50} (nM)	compound	R^3	IC_{50} (nM)
7 (DO130)	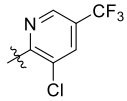	1100	**30**	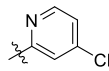	2100
22		>5000	**31**	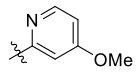	>5000
23	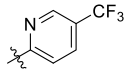	1900	**32**	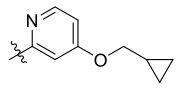	4700
24	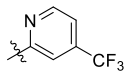	640	**33**	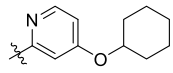	3400
25	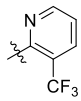	>5000	**34**	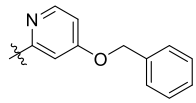	2800
26		630	**35**	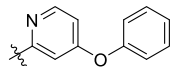	1900
27	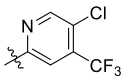	1400	**36**	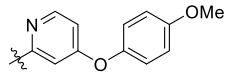	2900
28	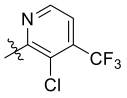	300	**37**	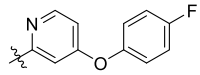	1400
29	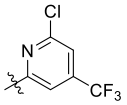	540	**38**	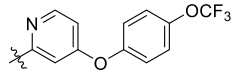	410

(Table 2). The importance of the CF_3 group was apparent, as its removal (**22**) abolished ABHD12 activity up to 5 μM. On the other hand, removal of the Cl group (**23**) resulted in only a small loss in potency. A CF_3 group ring scan revealed the 4- and 6-positions (**24** and **26**) were favorable for ABHD12 blockade relative to 5- and 3-positions (**23** and **25**), leading to the first submicromolar inhibitors in this series. The synthetic accessibility of 4-substituted pyridines led us to further explore this position over the 6-substituted analogues, which demonstrated comparable activity. Maintaining the CF_3 in the 4-position, we next scanned a Cl group across the remaining three positions of the pyridyl ring (**27**–**29**), finding 3-Cl substitution (**28**) to further enhance potency (ABHD12 IC_{50} = 300 nM).

We then wondered if the CF_3 group in the 4-position could be replaced to gain additional potency. Substituting the 4-CF_3 group with a chlorine (**30**) modestly decreased (~3-fold) ABHD12 inhibitory activity, while conversion to a methoxy group (**31**) had an even more deleterious effect. Interestingly, elaborating the 4-position with alkoxyl, benzyloxy, and phenoxy groups furnished a set of compounds (**32**–**35**) with superior activity to the 5-methoxy analogue (**31**) and revealed a scaffold trajectory that tolerated large substitutuents to potentially enhance potency. Given the superior ABHD12 inhibition of phenoxy analogue **35**, we introduced substitutents to the 4-position of the distal phenyl group and observed that while a methoxy group slightly impaired activity, fluoro (**37**) and especially OCF_3 (**38**) groups increased potency.

Identification of DO264 as a Potent and Selective ABHD12 Inhibitor. Having discovered that introducing an additional Cl group at the 3-position of the pyridine ring of **24** (**28**) or replacing the CF_3 group of **24** with a 4-OCF_3-phenyl group (**38**) improved ABHD12 inhibitory activity, we wondered

DOI: 10.1021/acs.jmedchem.8b01958
J. Med. Chem. XXXX, XXX, XXX−XXX

Table 3. SAR Leading to ABHD12 Chemical Probe DO264 (46)

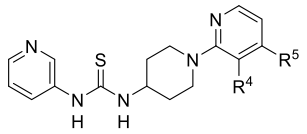

compound	R^4	R^5	IC_{50} (nM)	compound	R^4	R^5	IC_{50} (nM)
39	Cl	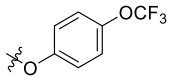	25	**43**	Cl	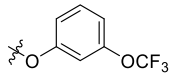	89
40	CH_3	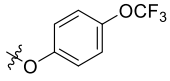	26	**44**	Cl	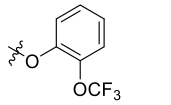	96
41	CN	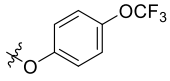	180	**45**	Cl	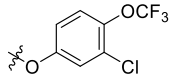	33
42	CF_3	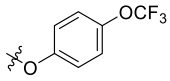	2800	**46** (DO264)	Cl	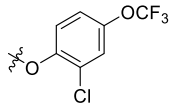	11

if these positive effects would be additive when combined into a single compound. Indeed, the hybrid compound **39** displayed dramatically increased ABHD12 inhibitory activity (>10-fold) compared to **28** or **38** (Table 3). Conversion of the Cl group of **39** to a methyl group (**40**) did not alter potency, but substitution at this position with a CN (**41**) or CF_3 (**42**) group reduced ABHD12 inhibitory activity, indicating that the Cl group contributed to potency primarily through a steric rather than electron withdrawing effect. The regioisomers of **39** bearing 3-OCF_3 (**43**) or 2-OCF_3 (**44**) groups showed ~3- to 4-fold lower potencies. Finally, introduction of a Cl group at the 2-position, but not the 3-position (**45**), of the distal phenyl provided another 2-fold increase in inhibitory activity to furnish DO264 (**46**), a highly potent (IC_{50} = 11 nM) ABHD12 inhibitor.

In the course of our SAR studies, we noted that compound **13** bearing a 3-aminopiperidine in place of the 4-aminopiperidine showed dramatically reduced ABHD12 inhibitory activity (Table 1B and Table 4). We capitalized on this observation to generate (S,R)-DO271 (**47**) (Table 4 and Figure 4), which showed a ~10 000-fold reduction in potency for ABHD12 inhibition compared to DO264. We found that (S)-DO271 (**48**) was less active than (R)-DO271 (**49**) (Table 4 and Figure 4) and therefore designated (S)-DO271 as an inactive control probe for biological studies. While it may seem surprising that neither enantiomer of DO271 appeared more potent than the racemate, we believe that this reflects the technical challenge of accurately measuring such weak IC_{50} values (>50 μM), especially as high concentrations of compound may approach their solubility limit.

ABPP studies of DO264 (**46**) and other representative (thio)urea inhibitors of ABHD12 confirmed that these compounds show excellent selectivity over other serine hydrolases (Figure 5),[19] including phosphatidylserine lipases, such PS-PLA1[27] and ABHD16A,[28] which contribute to lyso-PS production, and the PLA1-type PI lipase DDHD1 involved in lyso-PI production.[29] We also confirmed the activity and selectivity of DO264 in vivo, where the compound was found to produce substantial elevations in brain lyso-PS/PI and C20:4 PS content in mice.[19]

Table 4. Identification of an Inactive Control Probe (S)-DO271 (48)

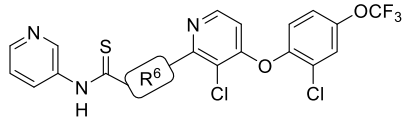

compound	R^6	IC_{50} (μM)
47 ((S, R)-DO271)	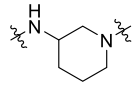	90
48 ((S)-DO271)	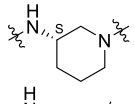	>100
49 ((R)-DO271)	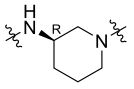	100

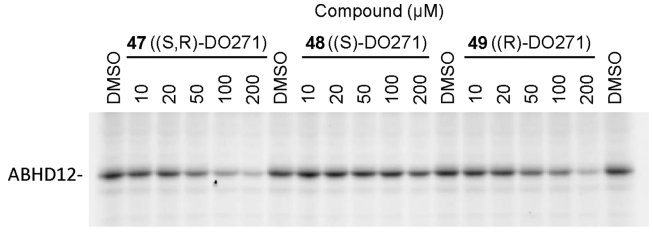

Figure 4. ABHD12 inhibitory activity of (S,R)-DO271 (**47**), (S)-DO271 (**48**), and (R)-DO271 (**49**) as measured by gel-based ABPP of mouse brain membrane proteome (1 mg/mL protein) using the JJH350 probe (2 μM, 45 min, 37 °C).

DOI: 10.1021/acs.jmedchem.8b01958
J. Med. Chem. XXXX, XXX, XXX−XXX

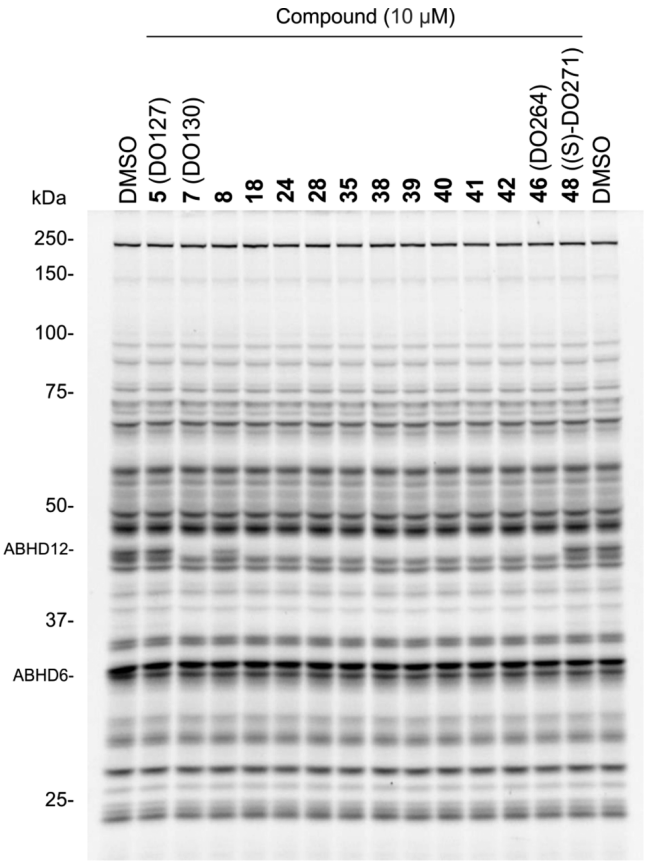

Figure 5. Gel-based ABPP of DO264 (**46**) and other representative (thio)urea inhibitors of ABHD12 in mouse brain membrane proteome using the FP-Rh probe (1 μM, 45 min, 37 °C).

ABHD12 Inhibition Modulates Cytokine Production in Human THP-1 Cells. Considering that ABHD12 is highly expressed in macrophages and microglia[17,18] and that genetic or pharmacological perturbation of ABHD12 produces heightened (neuro)immunological phenotypes in mice,[16,19,28] we next tested whether DO264 affected cytokine production using the human monocyte THP-1 cell line as a model system. THP-1 monocytes were first treated with phorbol 12-myristate 13-acetate (PMA) to produce resting macrophages characterized by changes in morphology and increased cell surface expression of CD11 and CD14.[30−32] Cells were allowed to rest for 24 h followed by polarization to the M1 stage with lipopolysaccharide (LPS) and IFN-γ. Each cell treatment step was performed in the presence of either DO264, (S)-DO271, or DMSO (Figure 6A). Consistent with previous studies of peritoneal macrophages from ABHD12(−/−) mice, which showed elevated TNF-α and IL-1β both basally and in response to LPS treatment,[28] the DO264-treated, but not (S)-DO271-treated, M1 stage THP-1 macrophages showed concentration-dependent increases in these cytokines (Figure 6B). The levels of inflammatory chemokines (CCL3 and CCL4) were also elevated by DO264 but not (S)-DO271 (Figure 6B). Importantly, these cytokine/chemokine changes occurred across a concentration range of DO264 that produced complete inhibition of ABHD12 and increases in lyso-PS/20:4 PS content in THP-1 cells.[19] In the course of these studies, we noticed that higher concentrations of DO264 ($\geq$5 μM) impaired the viability of THP-1 cells (Figure S4). Since full engagement of ABHD12 is observed at lower concentrations of DO264 (1 μM),[19] we believe that the cytotoxic effect is not due to inhibition of ABHD12 but rather another (as of yet) unidentified mechanism. We tested DO264 in a broader panel of cell lines and found that individual lines

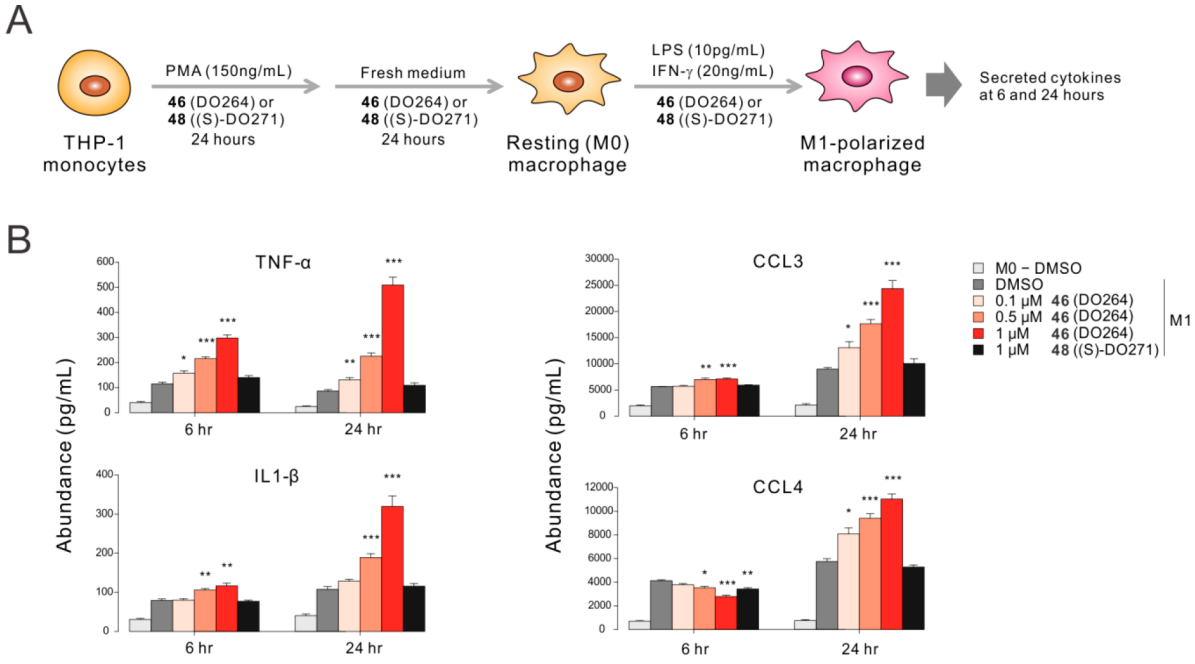

Figure 6. Concentration-dependent elevation of cytokines and chemokines in M1-polarized THP-1 macrophages treated with the ABHD12 inhibitor DO264. (A) PMA-differentiated THP-1 cells were polarized to M1 macrophages by stimulation with 20 ng/mL IFN-γ and 10 pg/mL LPS. (B) Cytokines and chemokines were measured 6 and 24 h after stimulation. DO264 and (S)-DO271 were included in the media at the specified concentrations throughout the experiment (A). Media samples from DMSO-treated resting (M0) macrophages were included as an additional control. Data represent the mean ± SEM from four independent biological experiments: (*) $p < 0.05$; (**) $p < 0.01$; (***) $p < 0.001$ (Student's t-test performed relative to M1-DMSO samples).

DOI: 10.1021/acs.jmedchem.8b01958
J. Med. Chem. XXXX, XXX, XXX−XXX

Scheme 1. Synthesis of 1−3[a]

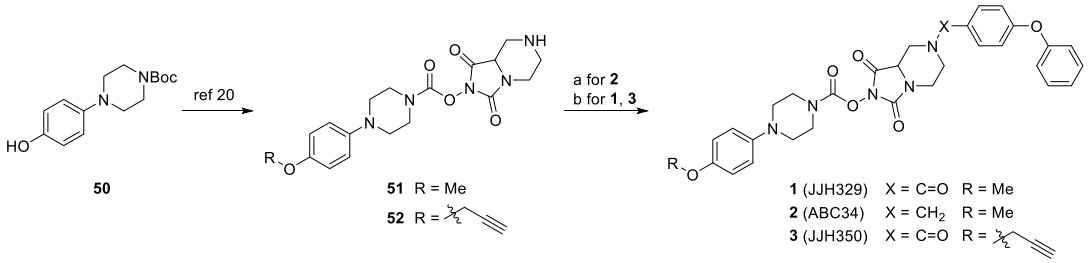

[a]Reagents and conditions: (a) 4-phenoxybenzaldehyde, acetic acid, $NaBH(OAc)_3$, dry THF, rt, 45% (ref 20); (b) 4-phenoxybenzoic acid, EDCI, $HOBt·H_2O$, iPr_2NEt_3, rt, 74% for **2**, 86% for **3**.

Scheme 2. Synthesis of 5−7[a]

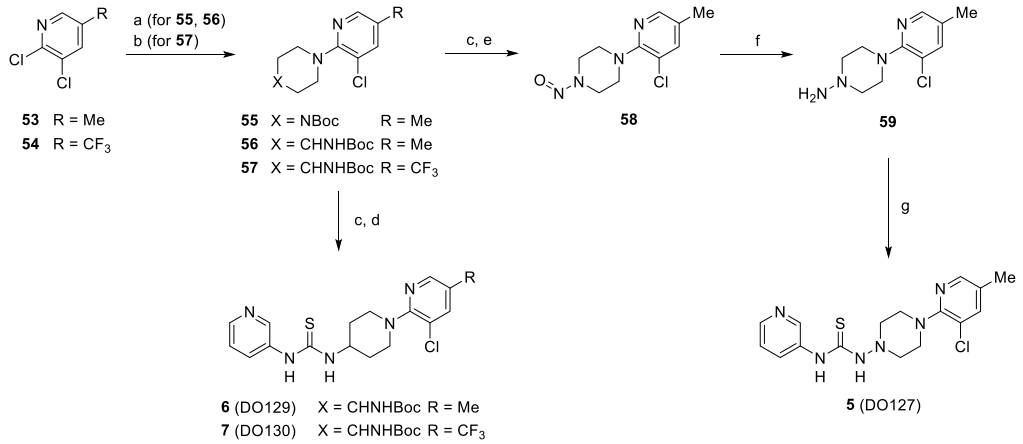

[a]Reagents and conditions: (a) Boc-amine, Cu powder, neat (for **55**) or dry DMF (for **56**), 120 °C, 64% for **55**, 37% for **56**; (b) *tert*-butyl (piperidin-4-yl)carbamate, K_2CO_3, dry DMSO, 100 °C, 91%; (c) 4 N HCl in 1,4-dioxane, CH_2Cl_2, rt; (d) pyridine-3-isothiocyanate, iPr_2NEt_3, CH_2Cl_2, rt, 75% for **6**, 94% for **7** (2 steps); (e) $NaNO_2$, acetic acid, H_2O, 0 °C to rt, 96% (2 steps); (f) Zn powder, MeOH/acetic acid, 0 °C to rt; (g) pyridine-3-isothiocyanate, iPr_2NEt_3, CH_2Cl_2, rt, 55% (2 steps).

showed variable degrees of sensitivity to the compound, but all of the cell lines could be treated with DO264 at 1 μM without displaying cytotoxicity (Figure S4). These data indicate that cellular studies performed with DO264 should not use greater than 1 μM compound, which is sufficient to fully inhibit ABHD12[19] without causing cytotoxicity. Finally, we should also note that the total exposure levels of DO264 can reach 3−9 μM in the periphery and brain of mice (30 mg/kg DO264, po or ip dosing), without overt signs of toxicity, even following treatment with the compound for several weeks.[19] This may indicate a much lower free fraction of DO264 at pharmacologically relevant doses or that the cytotoxicity observed for this compound in culture is not representative of the compound activity in vivo.

CONCLUSION

We have described herein an ABPP-guided medicinal chemistry program that culminated in the development of the first potent, selective, and in vivo active inhibitors of ABHD12, an enzyme responsible for hydrolyzing bioactive lyso-PS/PI lipids. We have shown that this compound, termed DO264, elevates lyso-PS/PI and C20:4 PS lipids in human cells and brain tissue of treated mice.[19] We also found that DO264-treated mice, as well as ABHD12(−/−) mice, show exacerbated immune responses to LCMV infection that included heightened chemokine production in vivo.[19] Consistent with a role for the ABHD12-(lyso)-PS/PI pathway in regulating immune cell activity, we found in this current study that DO264-treated THP-1 macrophages show heightened cytokine production. In future studies, it will be important to determine the specific (lyso)-PS/PI lipids and receptors involved in mediating the heightened immunological outcomes of ABHD12 blockade.

From a methodological perspective, the discovery of DO264 underscores the utilty of ABPP for developing not only irreversible but also reversible inhibitors of serine hydrolases, an attribute of the method that may be underappreciated, despite past examples of success.[21,33] Our program further benefited from the use of both general (FP-based) and tailored (JJH350) activity-based probes that enabled rigorous assessment of target engagement and selectivity for ABHD12 inhibitors, as well as the discovery of structurally related compounds that do not inhibit ABHD12 and can accordingly serve as inactive control probes (e.g., (S)-DO271). The toolbox of ABHD12-directed inhibitors and activity-based probes described herein should facilitate the pharmacological characterization of (lyso)-PS/PI pathways in mammalian biology and disease.

CHEMISTRY

The synthesis of *N*-hydroxyhydantoin carbamates **1** and **3** from commercially available piperazine **50** has been previously described (Scheme 1, refs 19 and 20). We used a similar route to prepare carbamate **2** where the common piperazine

DOI: 10.1021/acs.jmedchem.8b01958
J. Med. Chem. XXXX, XXX, XXX−XXX

intermediate (**51**) was subjected to amide coupling conditions with 4-phenoxybenzoic acid.

To prepare thiocarbamates **5**−**7**, methyl- or trifluoromethyl-chloropyridine (**53** or **54**, respectively) underwent 2-chloro substitution reactions with appropriate piperazines and piperidines by either a Cu-promoted amine cross-coupling (**55** and **56**) or SnAr reaction (**57**) (Scheme 2). Boc-deprotection of **56** and **57** followed by reaction of the resultant primary amines with pyridine-3-isothiocyanate gave thioureas **6** and **7**. To prepare semithiocarbazide **5**, the Boc group of piperazine **55** was first removed with HCl and the piperazine nitrosylated with $NaNO_2$. Subsequent nitroso reduction of **58** furnished hydrazine **59** which was then treated with pyridine-3-isothiocyanate to provide **5** (DO127) in 55% yield over two steps.

Analogues of DO130 featuring various 3-pyridylthiourea modifications each were accessible from common piperazine intermediate **57** (Scheme 3). Following Boc-deprotection of **57**,

Scheme 3. Synthesis of 8−12[a]

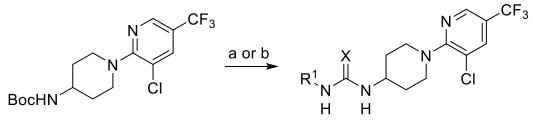

57 8-12

[a]Reagents and conditions: (a) 4 N HCl in 1,4-dioxane, CH_2Cl_2, rt, then R^1-NH_2, phenyl chlorothionoformate, iPr_2NEt_3, CH_2Cl_2, 21−45%; (b) 4 N HCl in 1,4-dioxane, CH_2Cl_2, rt, then R^1−N═C═S or R^1−N═ C═O, iPr_2NEt_3, CH_2Cl_2, rt, 71−100%.

thioureas **9**−**12** were prepared by either treating the free amine with *O*-phenyl chlorothionoformate and the indicated aromatic amines or, in the case of thiourea **12**, reacting the amine directly with phenylisothiocyanate. Similarly, urea **8** was synthesized through coupling deprotected **57** with pyridine-3-isocyanate.

Thioureas **13**−**31** with varying amine cores and pendant substituted pyridines were all prepared in a similar manner outlined Scheme 4. Chloropyridines **54** and **60a**−**j** were coupled

Scheme 4. Synthesis of 13−31[a]

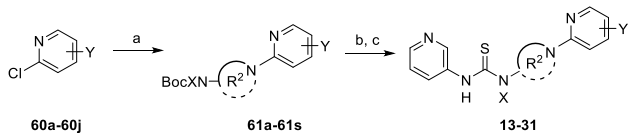

60a-60j 61a-61s 13-31

[a]Reagents and conditions: (a) Boc-amine, K_2CO_3, dry DMSO, 100 °C, 19−100%; (b) 4 N HCl in 1,4-dioxane, CH_2Cl_2, rt; (c) pyridine-3-isothiocyanate, iPr_2NEt_3, CH_2Cl_2, rt, 90−100% (2 steps).

with the appropriate Boc-protected diamines to give intermediates **61a**−**s** and subsequently deprotected. As described for previous analogues, the final thioureas (**13**−**31**) were obtained through treatment of the free amines with pyridine-3-isothiocyanate. For access to 4-alkoxy or 4-phenoxy substituted pyridines **67**−**81**, 2,4-dichloro- or 2-chloro-4-fluoropyridines were subjected to SnAr conditions in the presence of various alcohols and phenols which primarily displaced the halogen at the 4-position (Scheme 5). The remaining chloro group in the 2-position was displaced with *tert*-butyl (piperidin-4-yl)carbamate using similar SnAr conditions to provide **82**−**96**. Finally, thioureas **32**−**46** were obtained following Boc removal and coupling with pyridine-3-isothiocyanate. Inactive control compounds **47**−**49** were similarly prepared from 2-chloropyridine **81**.

EXPERIMENTAL SECTION

Chemistry. General Information. All chemical reagents were obtained from commercial suppliers and were used without further purification. Merck silica gel TLC plates (0.25 mm, 60 F254) were used to monitor reactions. Flash chromatography was performed using SiliaFlash F60 silica gel (40−63 μm, 60 Å). NMR spectra were recorded at room temperature on Bruker DRX-600 spectrometer at 600 (^{1}H) and 150 (^{13}C) MHz using $CDCl_3$ as solvent, unless stated otherwise. Chemical shifts are recorded in ppm relative to tetramethylsilane (TMS) with peaks being reported as follows: chemical shift, multiplicity (s = singlet, brs = broad singlet, d = doublet, t = triplet, q = quartet, m = multiplet), coupling constant (Hz). High-resolution mass spectra (HRMS) were obtained on an Agilent LC/MSD TOF mass spectrometer by electrospray ionization time-of-flight (ESI-TOF). The single crystal X-ray diffraction studies were carried out on a Bruker Kappa APEX-II CCD diffractometer equipped with Mo Kα radiation (λ = 0.71073 Å). Purities of all reported final compounds were determined to be greater than 95% measured by HPLC analysis (Waters Cortecs C18 column (2.1 mm × 55 mm, 1.6 mm) using a 0.1% aqueous formic acid/acetonitrile gradient (0.8 mL/min, 10−99% acetonitrile over 2.5 min, then 0.2 min isocratic hold) at 35 °C. The compounds were detected using UV light (MaxPlot over 220−400 nm). Enantiomeric excess (ee %) for compounds **48** and **49** were determined to be greater than 95% ee measured by Waters UPC2 SFC with a Daicel IBN column (3 μm, 4.6 mm × 250 mm) under isocratic conditions [40% MeOH/CO_2 (4 mL/min), 1600 psi backpressure] at 30 °C. The enantiomers were detected by UV light (257 nm).

1,3-Dioxo-7-(4-phenoxybenzoyl)hexahydroimidazo[1,5-*a*]-pyrazine-2(3*H*)-yl 4-(4-Methoxyphenyl)piperazine-1-carboxylate (1, JJH329). 1,3-Dioxohexahydroimidazo[1,5-*a*]pyrazin-2(3*H*)-yl 4-(4-methoxyphenyl)piperazine-1-carboxylate·2HCl (compound **51**·2HCl)[20] (42 mg, 92 μmol) was dissolved in 0.5 mL of DMF, and 4-phenoxybenzoic acid (24 mg, 110 μmol), 1-ethyl-3-(3-dimethylaminopropyl)carbodiimide hydrochloride (EDCI·HCl) (26 mg, 140 μmol), 1-hydroxybenzotriazole monohydrate (HOBt·H_2O) (21 mg, 140 μmol), *N*,*N*-diisopropylethylamine (48 μL, 270 μmol) were added. The resulting mixture was stirred at room temperature overnight and poured into saturated aqueous $NaHCO_3$ solution. The mixture was extracted with ethyl acetate (two times). The combined organic layer was washed with H_2O and brine, dried over Na_2SO_4, and concentrated under reduced pressure. The residue was purified by prep-TLC (ethyl acetate/hexane = 2:1) to afford **1** (JJH329) (40 mg, 74%) as a white solid. ^{1}H NMR ($CDCl_3$, 600 MHz) δ 7.44−7.36 (m, 4H), 7.19 (tt, J = 7.4, 1.1 Hz, 1H), 7.09−7.05 (m, 2H), 7.04−7.00 (m, 2H), 6.92−6.89 (m, 2H), 6.87−6.82 (m, 2H), 4.21−4.04 (m, 2H), 3.80 (brs, 2H), 3.77 (s, 3H), 3.67 (brs, 2H), 3.11 (brs, 8H). ^{13}C NMR ($CDCl_3$, 150 MHz) δ 170.83, 160.09, 155.85, 154.77, 151.00, 145.19, 130.16, 129.52, 128.35, 124.56, 120.10, 119.40, 118.14, 114.68, 55.66, 54.60, 50.78, 45.42, 44.82, 39.41. HRMS calculated for $C_{31}H_{32}N_5O_7$ $[M + H]^+$ 586.2302, found 586.2307.

***N*-3-Pyridyl-*N*′-[1-{3-chloro-5-(methyl)pyridin-2-yl}-piperidin-4-yl]thiourea (6, DO129).** To a solution of **56** (9.7 mg, 30 μmol) in DCM (0.1 mL) was added 4 N HCl in dioxane (0.1 mL) in a dropwise fashion, and the mixture was stirred for 2 h at room temperature. The mixture was dried under N_2 stream. The residue was dissolved in DCM (0.2 mL) with iPr_2NEt (21 μL, 0.12 mmol) and pyridine-3-isothiocyanate (4.5 mg, 30 μmol). The mixture was stirred for 17 h at room temperature. The mixture was diluted with DCM and washed with sat. $NaHCO_3$. The organic layer was dried over Na_2SO_4 and concentrated under reduced pressure. The residue was purified by preparative TLC (ethyl acetate only) to afford **6** (DO129) (8.1 mg, 75%) as a white solid. ^{1}H NMR ($CDCl_3$, 600 MHz) δ 8.56−8.47 (m, 2H), 7.95 (s, 1H), 7.81 (s, 1H), 7.63 (d, J = 7.5 Hz, 1H), 7.42−7.38 (m, 1H), 7.36 (d, 1H), 5.87 (s, 1H), 4.48 (s, 1H), 3.63 (d, 2H), 2.95 (t, 2H), 2.21 (s, 3H), 2.20−2.15 (m, 2H), 1.64−1.55 (m, 2H). ^{13}C NMR ($CDCl_3$, 150 MHz) δ 180.17, 156.64, 148.29, 146.62, 145.89, 139.51, 133.32, 132.71, 128.14, 124.58, 122.78, 52.68, 48.38, 31.81, 17.28.

DOI: 10.1021/acs.jmedchem.8b01958
J. Med. Chem. XXXX, XXX, XXX−XXX

Scheme 5. Synthesis of 32−49[a]

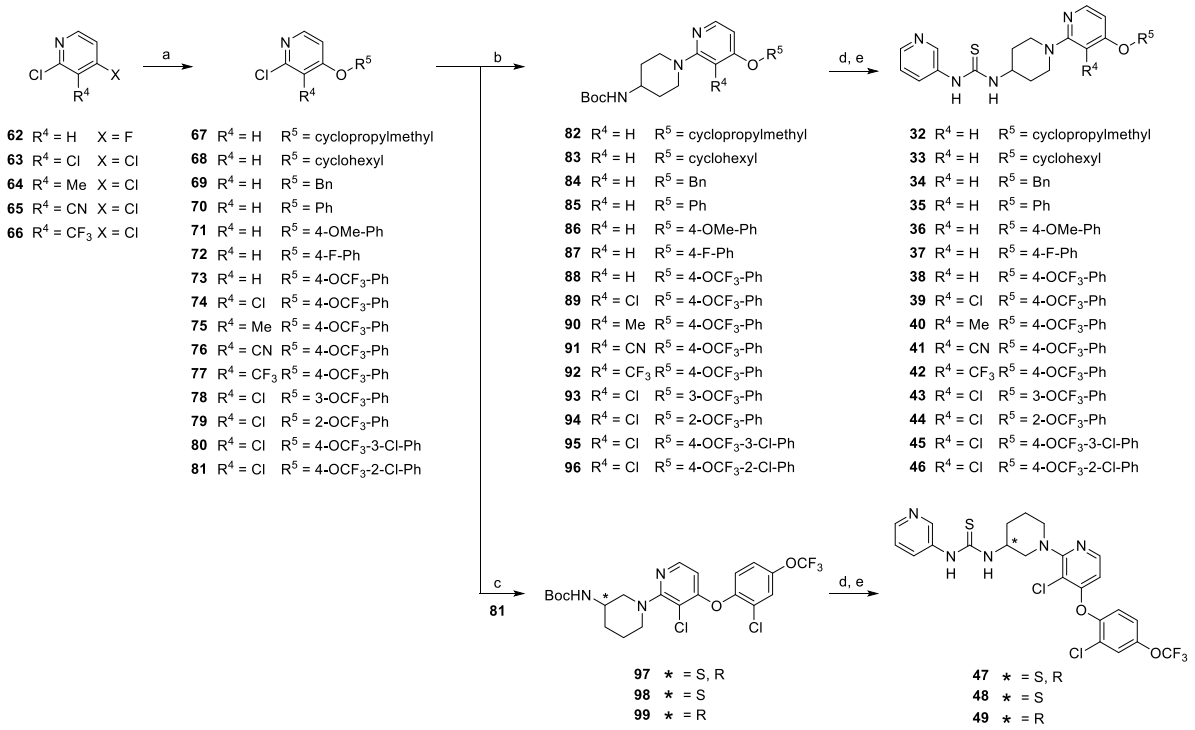

[a]Reagents and conditions: (a) R^5-OH, NaH in mineral oil, dry DMF, 0 °C then 90−100 °C, 61−100%; (b) *tert*-butyl (piperidin-4-yl)carbamate, K_2CO_3, dry DMSO, 100 °C, 20−94%; (c) *tert*-butyl (piperidin-3-yl)carbamate, K_2CO_3, dry DMSO, 100 °C, 45−51%; (d) 4 N HCl in 1,4-dioxane, CH_2Cl_2, rt; (e) pyridine-3-isothiocyanate, iPr_2NEt_3, CH_2Cl_2, rt, 78−100% (2 steps).

HRMS calculated for $C_{17}H_{21}ClN_5S$ $[M + H]^+$ 362.1206, found 362.1205.

***N*-{6-(methoxy)Pyridin-3-yl}-*N′*-[1-{3-chloro-5-(trifluoromethyl)pyridin-2-yl}piperidin-4-yl]thiourea (9).** Step 1: To a solution of a **57** (15 mg, 39 μmol) in DCM (0.1 mL) was added 4 N HCl in dioxane (0.1 mL) in a dropwise fashion, and the mixture was stirred for 2 h at room temperature. The mixture was dried under N_2 stream. The residue was dissolved in DCM and washed with aqueous 1 N NaOH. The organic layer was dried over Na_2SO_4 and concentrated under reduced pressure. The residue was used in the next step.

Step 2: To a solution of an 3-amino-6-methoxypyridine (5.3 mg, 42 μmol) in DCM with iPr_2NEt (27 μL, 150 μmol) was added phenyl chlorothioformate (7.3 mg, 42 μmol) at 0 °C, and the mixture was stirred for 2 h at room temperature. The Boc-deprotected amine obtained in step 1 was added, and the mixture was stirred overnight at room temperature. The mixture was diluted with DCM and washed with sat. $NaHCO_3$. The organic layer was dried over Na_2SO_4 and concentrated under reduced pressure. The residue was purified by prep-TLC (ethyl acetate/hexane = 1:2) to afford **9** (5.0 mg, 29%) as a colorless amorphous compound. ^{1}H NMR ($CDCl_3$, 600 MHz) δ 8.36 (s, 1H), 8.09−8.07 (m, 1H), 7.74−7.73 (m, 1H), 7.49 (s, 1H), 7.47−7.43 (m, 1H), 6.82 (d, 1H), 5.62−5.45 (m, 1H), 4.56 (s, 1H), 4.03−3.94 (m, 5H), 3.06 (t, 2H), 2.26−2.15 (m, 2H), 1.57−1.48 (m, 2H). ^{13}C NMR ($CDCl_3$, 150 MHz) δ 180.95, 163.64, 159.98, 145.41, 143.11, 137.53, 136.10, 125.85, 123.43 (q, $^1J_{C-F}$ = 269.9 Hz), 120.97, 120.10 (q, $^2J_{C-F}$ = 33.3 Hz), 112.58, 54.12, 52.64, 47.80, 31.78. HRMS calculated for $C_{18}H_{20}ClF_3N_5OS$ $[M + H]$+ 446.1029, found 446.1031.

***N*-3-Pyridyl-*N′*-[1-{3-chloro-5-(trifluoromethyl)pyridin-2-yl}piperidin-3-yl]thiourea (13).** To a solution of a **61a** (20 mg, 53 μmol) in DCM (0.2 mL) was added 4 N HCl in dioxane (0.2 mL) in a dropwise fashion, and the mixture was stirred for 2 h at room temperature. The mixture was dried under N_2 stream. The residue was dissolved in DCM with iPr_2NEt (37 μL, 0.21 mmol), and pyridine-3-isothiocyanate (7.9 mg, 58 μmol) was added. The mixture was stirred overnight at room temperature. The mixture was diluted with DCM and washed with sat. $NaHCO_3$. The organic layer was dried over Na_2SO_4 and concentrated under reduced pressure. The residue was purified by prep-TLC (AcOEt only) to afford **13** (24 mg, quantitative yield) as a white solid. ^{1}H NMR ($CDCl_3$, 600 MHz) δ 8.54 (s, 1H), 8.46 (d, 1H), 8.32 (s, 1H), 7.81 (s, 1H), 7.69 (s, 1H), 7.67−7.55 (m, 2H), 7.29 (d, 1H), 4.66 (s, 1H), 3.82−3.62 (m, 2H), 3.30 (s, 1H), 3.15 (s, 1H), 2.32 (s, 1H), 1.95−1.58 (m, 3H). ^{13}C NMR ($CDCl_3$, 150 MHz) δ 180.16, 160.03, 147.96, 146.68, 142.74, 136.40, 133.70, 132.58, 124.43, 123.12 (q, $^1J_{C-F}$ = 270.2 Hz), 122.00, 120.59 (q, $^2J_{C-F}$ = 33.5 Hz), 120.42, 52.56, 50.99, 49.97, 28.27, 22.15. HRMS calculated for $C_{17}H_{18}ClF_3N_5S$ $[M + H]^+$ 416.0924, found 416.0927.

***N*-3-Pyridyl-*N′*-[1-{4-(cyclopropylmethoxy)pyridin-2-yl}-piperidin-4-yl]thiourea (32).** To a solution of **82** (16 mg, 45 μmol) in DCM (0.2 mL) was added 4 N HCl in dioxane (0.2 mL) in a dropwise fashion, and the mixture was stirred for 2 h at room temperature. The mixture was dried under N_2 stream. The residue was dissolved in DCM with iPr_2NEt (39 μL, 0.22 mmol), and pyridine-3-isothiocyanate (8.4 mg, 62 μmol) was added. The mixture was stirred overnight at room temperature. The mixture was diluted with DCM and washed with sat. $NaHCO_3$. The organic layer was dried over Na_2SO_4 and concentrated under reduced pressure. The residue was purified by prep-TLC (DCM/acetone = 2/3) to afford **32** (16 mg, 95%) as a white solid. ^{1}H NMR ($CDCl_3$, 600 MHz) δ 8.49 (s, 3H), 7.96 (d, 1H), 7.77 (s, 1H), 7.35 (s, 1H), 6.40−6.19 (m, 2H), 6.10 (s, 1H), 4.52 (s, 1H), 4.12 (d, 2H), 3.79 (d, 2H), 2.98 (t, 2H), 2.19−2.06 (m, 2H), 1.40 (s, 2H), 1.27−1.19 (m, 1H), 0.67−0.61 (m, 2H), 0.36−0.30 (m, 2H). ^{13}C NMR ($CDCl_3$, 150 MHz) δ 180.38, 166.99, 161.01, 149.09, 101.54, 93.04, 72.62, 52.60, 44.82, 31.20, 10.10, 3.36. HRMS calculated for $C_{20}H_{26}N_5OS$ $[M + H]^+$ 384.1858, found 384.1861.

***N*-3-Pyridyl-*N′*-(1-[3-methyl-4-{4-(trifluoromethoxy)-phenoxy}pyridine-2-yl]piperidin-4-yl)thiourea (40).** To a solution of **90** (20 mg, 43 μmol) in DCM (0.2 mL) was added 4 N HCl in dioxane (0.2 mL) in a dropwise fashion, and the mixture was stirred for 2 h at room temperature. The mixture was dried under N_2 stream. The residue was dissolved in DCM with iPr_2NEt (30 μL, 0.17 mmol), and pyridine-3-isothiocyanate (6.4 mg, 47 μmol) was added. The mixture was stirred overnight at room temperature. The mixture was diluted

DOI: 10.1021/acs.jmedchem.8b01958
J. Med. Chem. XXXX, XXX, XXX−XXX

with DCM and washed with sat. $NaHCO_3$. The organic layer was dried over Na_2SO_4 and concentrated under reduced pressure. The residue was purified by prep-TLC (DCM/acetone = 3/1) to afford **40** (25 mg, quantitative yield) as a colorless amorphous compound. ^{1}H NMR ($CDCl_3$, 600 MHz) δ 8.58−8.49 (m, 2H), 8.04−7.98 (m, 1H), 7.89 (s, 1H), 7.72 (s, 1H), 7.39 (s, 1H), 7.22 (d, 2H), 7.02 (d, 2H), 6.33 (d, 1H), 6.06 (s, 1H), 4.53 (s, 1H), 3.49−3.34 (m, 2H), 3.09−2.93 (m, 2H), 2.29−2.08 (m, 5H), 1.50−1.32 (m, 2H). ^{13}C NMR ($CDCl_3$, 600 MHz) δ 180.08, 163.60, 162.32, 153.96, 146.08, 144.68, 144.42, 136.39, 130.18, 123.11, 120.88, 120.09 (q, $^1J_{C-F}$ = 254.4 Hz), 113.87, 107.03, 50.75, 48.68, 31.17, 11.26. HRMS calculated for $C_{24}H_{25}F_3N_5O_2S$ $[M + H]^+$ 504.1681, found 504.1677.

(*R*)-*N*-3-Pyridyl-*N*′-(1-[3-chloro-4-{3-chloro-4-(trifluoromethoxy)phenoxy}pyridine-2-yl]piperidin-3-yl)-thiourea (49). To a solution of **99** (20 mg, 38 μmol) in DCM (0.2 mL) was added 4 N HCl in dioxane (0.2 mL) in a dropwise fashion, and the mixture was stirred for 2 h at room temperature. The mixture was dried under N_2 stream. The residue was dissolved in DCM with iPr_2NEt (27 μL, 0.15 mmol), and pyridine-3-isothiocyanate (5.7 mg, 42 μmol) was added. The mixture was stirred overnight at room temperature. The mixture was diluted with DCM and washed with sat. $NaHCO_3$. The organic layer was dried over Na_2SO_4 and concentrated under reduced pressure. The residue was purified by prep-TLC (DCM/acetone = 3/1) to afford **49** (12 mg, 57%) as a colorless amorphous compound. ^{1}H NMR ($CDCl_3$, 600 MHz) δ 8.56 (s, 1H), 8.46 (dd, J = 4.8, 1.5 Hz, 1H), 7.83 (s, 2H), 7.62 (s, 1H), 7.54 (s, 1H), 7.40 (d, J = 2.8 Hz, 1H), 7.30 (dd, J = 8.1, 4.7 Hz, 1H), 7.20 (dd, J = 8.9, 2.8 Hz, 1H), 7.13 (d, J = 8.9 Hz, 1H), 6.09 (d, J = 5.6 Hz, 1H), 4.76−4.06 (m, 1H), 3.79−2.81 (m, 4H), 2.35 (s, 1H), 1.70 (s, 3H). ^{13}C NMR ($CDCl_3$, 150 MHz) δ 179.99, 160.68, 160.52, 148.64, 147.93, 146.65, 146.59, 146.03, 133.71, 132.51, 127.86, 124.50, 124.07, 123.31, 121.16, 120.42 (q, $^1J_{C-F}$ = 257.0 Hz), 111.95, 106.05, 53.32, 51.10, 50.68, 28.23, 21.97. HRMS calculated for $C_{23}H_{20}Cl_2F_3N_5O_2S$ $[M + H]^+$ 558.0745, found 558.0755.

***tert*-Butyl [1-{3-Chloro-5-methylpyridin-2-yl}piperidin-4-yl]-carbamate (56).** A solution of 2,3-dichloro-5-(methyl)pyridine (**53**) (200 mg, 1.23 mmol), *tert*-butyl (piperidin-4-yl)carbamate (2.5 g, 12 mmol), and Cu powder (8 mg) in DMF (4 mL) was stirred for 18 h at 120 °C. The mixture was diluted with DCM and filtered through a silica pad (ethyl acetate/hexane = 1:1 as an eluent). The eluent was concentrated under reduced pressure. The residue was purified by flash column chromatography (hexane only, then ethyl acetate/hexane = 1:10 to 1:3) to afford **56** (150 mg, 37%) as a yellow amorphous compound. ^{1}H NMR ($CDCl_3$, 600 MHz) δ 7.92 (d, J = 1.9 Hz, 1H), 7.35 (d, J = 2.0 Hz, 1H), 4.59 (d, J = 8.2 Hz, 1H), 3.65−3.52 (m, 3H), 2.84 (ddd, J = 13.2, 11.3, 2.5 Hz, 2H), 2.16 (s, 3H), 2.01−1.94 (m, 2H), 1.52 (dtd, J = 12.6, 11.0, 3.9 Hz, 2H), 1.34 (s, 9H). ^{13}C NMR ($CDCl_3$, 150 MHz) δ 156.82, 155.22, 145.71, 139.31, 127.76, 122.72, 79.20, 48.47, 47.83, 32.60, 28.46, 17.15. ESI-MS 326.1: ($[M + H]^+$).

***tert*-Butyl [1-{3-Chloro-5-(trifluoromethyl)pyridin-2-yl}-piperidin-3-yl]carbamate (61a).** A solution of 2,3-dichloro-5-trifluoromethylpyridine (**54**) (200 mg, 0.93 mmol), *tert*-butyl (piperidin-3-yl)carbamate (220 mg, 1.1 mmol), and potassium carbonate (130 mg, 0.93 mmol) in dry DMF (0.5 mL) was stirred at 100 °C overnight. The mixture was diluted with DCM and filtered through a pad of silica with ethyl acetate. The eluent was concentrated under reduced pressure and the residue was purified by flash column chromatography (ethyl acetate/hexane = 1/8 to 1/3) to afford **61a** (350 mg, 99%) as a white solid. ^{1}H NMR ($CDCl_3$, 600 MHz) δ 8.33 (s, 1H), 7.70 (d, J = 2.3 Hz, 1H), 5.14−4.79 (m, 1H), 3.89−3.03 (m, 5H), 1.87−1.74 (m, 2H), 1.74−1.50 (m, 2H), 1.39 (s, 9H). ^{13}C NMR ($CDCl_3$, 150 MHz) δ 160.52, 155.21, 142.98, 135.96, 123.35 (q, $^1J_{C-F}$ = 269.9 Hz), 121.47, 120.16 (q, $^2J_{C-F}$ = 33.2 Hz), 79.25, 53.80, 49.51, 46.52, 29.99, 28.42, 22.54. ESI-MS: 380.1 ($[M + H]^+$).

2-Chloro-4-(cyclopropylmethoxy)pyridine (67). To a solution of 2-cyclopropylmethanol (160 mg, 2.3 mmol) in dry DMF (1 mL) was slowly added 60% sodium hydride in mineral oil (91 mg, 2.3 mmol) at 0 °C. The mixture was warmed to room temperature and stirred for 20 min. The reaction mixture was added 4-fluoropyridine (**62**) (300 mg, 2.3 mmol). The reaction mixture was stirred at 90 °C, and the reaction was stirred overnight. The reaction mixture was concentrated under reduced pressure. The residue was purified by flash column chromatography (hexane only and then to ethyl acetate/hexane = 1/8) to afford **67** (290 mg, 70%) as a colorless oil. ^{1}H NMR ($CDCl_3$, 600 MHz) δ 8.09 (d, J = 5.8 Hz, 1H), 6.75 (d, J = 2.3 Hz, 1H), 6.68 (dd, J = 5.8, 2.3 Hz, 1H), 3.79 (d, J = 7.1 Hz, 2H), 1.23−1.16 (m, 1H), 0.64−0.57 (m, 2H), 0.34−0.27 (m, 2H). ^{13}C NMR ($CDCl_3$, 150 MHz) δ 166.60, 152.51, 150.18, 110.11, 109.86, 73.22, 9.75, 3.31. ESI-MS 184.1: ($[M + H]^+$).

2-Chloro3-methyl-4-{4-(trifluoromethoxy)phenyloxy}-pyridine (75). To a solution of 4-(trifluoromethoxy)phenol (60 mg, 0.34 mmol) in dry DMF (0.2 mL) was slowly added 60% sodium hydride in mineral oil (14 mg, 0.34 mmol) at 0 °C. The mixture was warmed to room temperature and stirred for 20 min. To the he reaction mixture was added 2,4-dichloro-3-methylpyridine (**64**) (50 mg, 0.31 mmol). The reaction mixture was stirred at 120 °C, and the reaction was stirred overnight. The reaction mixture was concentrated under reduced pressure. The residue was purified by prep-TLC (ethyl acetate/hexane = 1/10) to afford **75** (59 mg, 63%) as a colorless oil. ^{1}H NMR ($CDCl_3$, 600 MHz) δ 8.08 (d, J = 5.6 Hz, 1H), 7.31−7.26 (m, 2H), 7.11−7.06 (m, 2H), 6.56 (d, J = 5.6 Hz, 1H), 2.40 (s, 3H). ^{13}C NMR ($CDCl_3$, 150 MHz) δ 163.81, 153.36, 153.00, 147.60, 146.19, 123.13, 122.74, 121.55, 120.53 (q, $^1J_{C-F}$ = 255.5 Hz), 110.16, 12.58. ESI-MS 304.0: ($[M + H]^+$).

***tert*-Butyl [1-{4-(Cyclopropylmethyloxy)pyridin-2-yl}-piperidin-4-yl]carbamate (82).** A solution of **67** (80 mg, 0.44 mmol), *tert*-butyl (piperidin-4-yl)carbamate (440 mg, 2.2 mmol), and potassium carbonate (120 mg, 0.87 mmol) in dry DMSO (1 mL) was stirred at 120 °C for 24 h. The mixture was diluted with DCM and filtered through a pad of silica with ethyl acetate. The eluent was concentrated under reduced pressure and the residue was purified by flash column chromatography (hexane only and then to hexane/ethyl acetate = 1/10 to 1/2) to afford **82** (40 mg, 26%) as a white solid. ^{1}H NMR ($CDCl_3$, 600 MHz) δ 7.99 (d, J = 5.8 Hz, 1H), 6.20 (dd, J = 5.8, 2.1 Hz, 1H), 6.11 (d, J = 2.1 Hz, 1H), 4.54−4.42 (m, 1H), 4.14 (dt, J = 13.9, 3.6 Hz, 2H), 3.79 (d, J = 7.0 Hz, 2H), 3.72−3.60 (m, 1H), 2.93 (ddd, J = 13.8, 11.6, 2.7 Hz, 2H), 2.04−1.94 (m, 2H), 1.49−1.34 (m, 11H), 1.28−1.18 (m, 1H), 0.68−0.60 (m, 2H), 0.37−0.29 (m, 2H). ^{13}C NMR ($CDCl_3$, 150 MHz) δ 166.79, 161.26, 155.28, 149.22, 101.22, 92.77, 79.46, 72.48, 48.29, 44.72, 32.21, 28.52, 10.13, 3.33. ESI-MS 348.2: ($[M + H]^+$).

***tert*-Butyl (1-[3-Methyl-4-{4-(trifluoromethoxy)phenoxy}-pyridine-2-yl]piperidin-4-yl)carbamate (90).** A solution of **75** (120 mg, 0.37 mmol), *tert*-butyl(piperidin-4-yl)carbamate (300 mg, 1.5 mmol), and potassium carbonate (80 mg, 0.56 mmol) in dry DMSO (0.2 mL) was stirred at 120 °C for 1 h. The mixture was diluted with DCM and filtered through a pad of silica with ethyl acetate. The eluent was concentrated under reduced pressure and the residue was purified by prep-TLC (ethyl acetate/hexane = 1/7) to afford **90** (64 mg, 37%) as a white solid. ^{1}H NMR ($CDCl_3$, 600 MHz) δ 8.01 (d, J = 5.6 Hz, 1H), 7.22−7.17 (m, 2H), 7.03−6.98 (m, 2H), 6.32 (d, J = 5.6 Hz, 1H), 4.57 (d, J = 8.1 Hz, 1H), 3.71−3.59 (m, 1H), 3.44−3.36 (m, 2H), 2.96−2.86 (m, 2H), 2.19 (s, 3H), 2.09−2.00 (m, 2H), 1.56 (dtd, J = 12.6, 10.9, 3.8 Hz, 2H), 1.44 (s, 9H). ^{13}C NMR ($CDCl_3$, 150 MHz) δ 164.26, 163.12, 155.32, 154.04, 146.12, 145.40, 122.86, 120.75, 120.57 (q, $^1J_{C-F}$ = 256.1 Hz), 114.83, 107.07, 79.41, 49.13, 47.96, 32.94, 28.39, 11.50. ESI-MS 468.1: ($[M + H]^+$).

(*R*)-*tert*-Butyl (1-[3-Chrolo-4-{2-chloro-4-(trifluoromethoxy)-phenoxy}pyridine-2-yl]piperidin-3-yl)carbamate (99). A solution of **81**[19] (120 mg, 0.37 mmol), (*R*)-*tert*-butyl (piperidin-3-yl)carbamate (150 mg, 0.74 mmol), and potassium carbonate (61 mg, 0.44 mmol) in dry DMSO (0.3 mL) was stirred at 100 °C for 3 h. The mixture was diluted with DCM and filtered through a pad of silica with ethyl acetate. The eluent was concentrated under reduced pressure and the residue was purified by prep-TLC (ethyl acetate/hexane = 1/3) to afford **99** (91 mg, 47%) as a white solid. ^{1}H NMR ($CDCl_3$, 600 MHz) δ 8.00 (d, J = 5.6 Hz, 1H), 7.39 (d, J = 2.8, 1H), 7.18 (dd, J = 8.9, 2.8, 1H), 7.13 (d, J = 9.0 Hz, 1H), 6.19 (d, J = 5.6 Hz, 1H), 5.33−4.89 (m, 1H), 3.97−3.65 (m, 1H), 3.51−3.08 (m, 4H), 1.92−1.59 (m, 4H), 1.44 (s, 9H). ^{13}C NMR ($CDCl_3$, 150 MHz) δ 161.17, 160.46, 155.40, 148.96, 146.38, 146.30, 127.78, 124.03, 123.07, 121.09, 120.42 (q, $^1J_{C-F}$

DOI: 10.1021/acs.jmedchem.8b01958
J. Med. Chem. XXXX, XXX, XXX−XXX

= 257.0 Hz), 111.94, 106.05, 79.28, 54.62, 50.43, 46.50, 29.99, 28.58, 22.51. ESI-MS 522.0: ($[M + H]^+$).

Lyso-PS Hydrolysis Assay. The lyso-PS lipase activity of ABHD12 was determined as described.[19] Briefly, DO127 was incubated with ABHD12-overexpressing HEK293T membrane (0.25 mg/mL) in DPBS for 20 min at room temperature. 17:1 lyso-PS in DPBS was added to each reaction (100 μM final concentration) and incubated at 37 °C. After 30 min, the reaction was quenched with 400 μL of 2:1 $CHCl_3$/MeOH (v/v) with 1 nmol of 15:0 FFA as an internal standard. The mixture was vortexed and centrifuged at 1400*g* to separate the aqueous and organic phase. The organic phase was analyzed by LC–MS (1200 LC/MSD, Agilent Technologies) using a 50 mm × 4.6 mm, 5 μm Gemini C18 column (Phenomenex) coupled to a guard column (Gemini C18, 4 mm × 3 mm). The LC solvents were as follows: buffer A, H_2O/MeOH (95:5, v/v) with 0.1% NH_4OH (v/v); buffer B, iPrOH/MeOH/H_2O (60:35:5, v/v/v) with 0.1% NH_4OH (v/v). The LC method consisted of 0.1 mL/min 20% buffer B for 1.0 min, 0.4 mL/min isocratic mode of 100% buffer B over 7 min, and equilibration with 0.5 mL/min 100% buffer A for 3 min. The MS analyses were performed using an electrospray ionization source (ESI) in negative ion mode to measure product formation. MS data were acquired in selected ion monitoring mode at *m*/*z* 267.20 for 17:1 FFA and *m*/*z* 241.20 for 15:0 FFA.

Gel-Based Competitive ABPP. Gel-based ABPP assays were performed as described.[19] Tissue proteomes (50 μL, 1 mg/mL) were treated with inhibitors for 20 min at room temperature (for (thio)urea analogues) or 45 min at 37 °C (for NHH carbamate analogues). Then the proteomes were labeled with FP-Rh (1 μM final concentration) or JJH350 (2 μM final concentration) for 45 min at 37 °C. For FP-Rh labeled samples, the reactions were quenched by adding 20 μL of 4× SDS–PAGE loading buffer. An amount of 30 μL of the quenched samples was loaded on gel for analysis. For JJH350-labeled samples, copper-catalyzed azide–alkyne cycloaddition (CuAAC) was used for visualizing the labeled proteins. For CuAAC, rhodamine-PEG_3-N_3 (1 μL/reaction, 1.25 mM in DMSO), $CuSO_4$ (1 μL/reaction, 50 mM in H_2O), TBTA (3 μL/reaction, 1.7 mM in DMSO/*t*-BuOH [1:4, v/v]) and tris(2-carboxyethyl)phosphine (TCEP) (1 μL/reaction, 50 mM in H_2O, freshly prepared) were premixed. Then 6 μL of this click reagents mixture was immediately added to each JJH350-labeled sample (50 μL, 1 mg/mL) and incubated for 1 h at room temperature. The reactions were quenched by adding 20 μL of 4× SDS–PAGE loading buffer. An amount of 40 μL of the quenched samples was loaded on a gel for analysis. After separation by SDS–PAGE (10% acrylamide), samples were visualized by in-gel fluorescence scanning using the ChemiDoc MP system (Bio-Rad). Band intensities were quantified using the Image Lab (5.2.1) software (Bio-Rad).

Preparation of Tissue Proteomes. Mouse tissues were dounce-homogenized in DPBS followed by low-speed spin (1400*g*, 3 min, 4 °C) to remove debris. The membrane and cytosolic fractions were separated by high-speed spin (16 000*g*, 45 min, 4 °C) of the resulting homogenate lysate. After removal of the soluble supernatant, the membrane pellet was washed with cold DPBS and resuspended with cold DPBS. Total protein concentrations in membrane fractions were determined using the Bio-Rad DC protein assay kit. Samples were used immediately for the following ABPP experiments.

IC_{50} Calculations. ABHD12 enzyme activities in mice brain membrane fraction were determined by fluorescent ABHD12 band intensity visualized by JJH350 probe followed by conjugation of rhodamine-N_3 (for detail, see gel-based competitive ABPP section). The relative intensity was compared to the ABHD12 band intensity from a control-treated sample, which was set to 100%. IC_{50} values were determined by plotting a log(inhibitor) vs normalized response, and the dose–response curves were generated using the Prism software (GraphPad).

Cytokine Measurements in THP-1 Cells. THP-1 cells (ATCC) were cultured in RPMI 1640 (Corning) with 10% heat-inactivated FBS (Omega Scientific) and 0.05 mM 2-mercaptoethanol (Fisher) at a density between 2×10^5 to 1×10^6 cells/mL. On day of experiment, cells were plated into 6-well culture plates at a concentration of 2.5×10^6 cells/well and treated with 150 ng/mL of phorbol 12-myristate 13-acetate (PMA, Sigma) for 24 h in the presence of DO264 (1, 0.5, and 0.1 μM), (S)-DO271 (1 μM), or DMSO. Following PMA treatment cells were adherent and washed twice with culture media to remove PMA. Cells were allowed to rest for 24 h to become resting macrophages in the presence of DO264, (S)-DO271, or DMSO. Resting macrophages were treated with fresh media containing 20 ng/mL IFN-γ (Sigma) and 10 pg/mL LPS (Sigma) for 24 h in the presence of DO264, (S)-DO271, or DMSO to achieve M1 polarization. Aliquots of media were collected 6 and 24 h following the addition of polarizing cytokines, and selected cytokines were measured using the MSD V-Plex Plus assay.

Cell Viability Assay. Cells were seeded into 96-well plates at 3000 cells per well. After 24 h, test compounds were added to cells to final concentrations ranging from 0.1 to 10 μM. Cells were then incubated for 72 h and cell viability was measured using CellTiter-Glo assay (Promega) following manufacturer's instructions. Relative cell viability in the presence of test compounds was normalized to the vehicle-treated controls.

Compound Treatment for in Vivo Studies. JJH329 was suspended in 1:1 (v/v) solution of EtOH/PEG40 (by bath sonication), and the solution was diluted with 9 volumes of DPBS followed by vortexing to obtain 1:1:18 (v/v/v) compound solution of EtOH/PEG40/DPBS. 10 μL/g mouse body weight of the freshly prepared compound solution was injected into the mouse peritoneal. Compound-treated mice were anesthetized with isoflurane and euthanized by cervical dislocation to harvest tissues. The experiments were conducted in accordance with the guidelines of the Institutional Animal Care and Use Committee of The Scripps Research Institute.

Statistics. Statistical analyses were performed using the R statistical programming language or Prism. All data are shown as mean values ± SEM or SD. Two-sided Student's *t* test was used to perform statistical analyses. A *p*-value of <0.05 was considered statistically significant for this study.

■ ASSOCIATED CONTENT

Supporting Information

The Supporting Information is available free of charge on the ACS Publications website at DOI: 10.1021/acs.jmedchem.8b01958.

Gel-based ABPP assay of JJH329-treated mice tissues, substrate assay data for DO127, ^{13}C NMR analysis of commercial AW01275, cytotoxicity assay of DO264, additional synthetic chemistry procedures and analytical data for compounds **8**, **10**–**12**, **14**–**31**, **33**–**37**, **41**–**45**, **47**, and X-ray crystallographic data summary for commercial AW01275 (PDF)

Molecular formula strings (CSV)

X-ray crystallographic data for commercial AW01275 (CIF)

■ AUTHOR INFORMATION

Corresponding Authors

*D.O.: e-mail, daisuke@scripps.edu.

*B.F.C.: e-mail, cravatt@scripps.edu.

ORCID

Benjamin F. Cravatt: 0000-0001-5330-3492

Notes

The authors declare the following competing financial interest(s): Dr. Cravatt is a co-founder and scientific advisor for Abide Therapeutics, a biotechnology company interested in developing serine hydrolase inhibitors as therapeutics.

■ ACKNOWLEDGMENTS

We thank M. Niphakis (Abide Therapeutics) for critical reading of the manuscript; J. Chen (Automated Synthesis Facility at

DOI: 10.1021/acs.jmedchem.8b01958
J. Med. Chem. XXXX, XXX, XXX–XXX

Scripps Research) for measuring purity of ABHD12 inhibitors; C. E. Moore and M. Gembicky (UCSD) for X-ray crystallographic analysis of AW01275. This work was supported by the NIH (Grants DA033760, NS092980) and Abide Therapeutics.

■ ABBREVIATIONS USED

ABHD12, α/β-hydrolase domain-containing 12; PHARC, polyneuropathy, hearing loss, ataxia, retinosa pigmentosa, and cataract; PS, phosphatidylserine; PI, phosphatidylinositol; GPCR, G-protein-coupled receptor; S1P, sphingosine 1-phosphate; PA, phosphatidic acid; CNS, central nervous system; ABPP, activity-based protein profiling; LCMV, lymphocytic choriomeningitis virus; SAR, structure−activity relationship; NHH, *N*-hydroxyhydantoin; FP-Rh, fluorophosphonate-rhodamine; ABHD6, α/β-hydrolase domain-containing 6; CI, confidence interval; CuAAC, copper-catalyzed azide−alkyne cycloaddition; Rh-N_3, rhodamine-$(PEG)_3$-azide; HTS, high-throughput screening; PMA, phorbol 12-myristate 13-acetate; LPS, lipopolysaccharide; IFN-γ, interferon γ; TNF-α, tumor necrosis factor-α; IL-1β, interleukin-1β; CCL3, chemokine ligand 3; CCL4, chemokine ligand 4; SnAr, nucleophilic aromatic substitution; EDCI, *N*-(3-dimethylaminopropyl)-*N*′-ethylcarbodiimide; HOBt, hydroxybenzotriazole; FFA, free fatty acid; TBTA, tris[(1-benzyl-1*H*-1,2,3-triazol-4-yl)methyl]-amine; TCEP, tris(2-carboxyethyl)phosphine; FBS, fetal bovine serum; SEM, standard error of the mean; SD, standard deviation

■ REFERENCES

(1) Grzelczyk, A.; Gendaszewska-Darmach, E. Novel Bioactive Glycerol-Based Lysophospholipids: New Data – New Insight into Their Function. *Biochimie* **2013**, *95* (4), 667−679.

(2) Makide, K.; Kitamura, H.; Sato, Y.; Okutani, M.; Aoki, J. Emerging Lysophospholipid Mediators, Lysophosphatidylserine, Lysophosphatidylthreonine, Lysophosphatidylethanolamine and Lysophosphatidylglycerol. *Prostaglandins Other Lipid Mediators* **2009**, *89* (3−4), 135−139.

(3) Yung, Y. C.; Stoddard, N. C.; Chun, J. LPA Receptor Signaling: Pharmacology, Physiology, and Pathophysiology. *J. Lipid Res.* **2014**, *55* (7), 1192−1214.

(4) Rosen, H.; Germana Sanna, M.; Gonzalez-Cabrera, P. J.; Roberts, E. The Organization of the Sphingosine 1-Phosphate Signaling System. *Curr. Top. Microbiol. Immunol.* **2014**, *378*, 1−21.

(5) Adams, D. R.; Pyne, S.; Pyne, N. J. Sphingosine Kinases: Emerging Structure-Function Insights. *Trends Biochem. Sci.* **2016**, *41* (5), 395−409.

(6) Castagna, D.; Budd, D. C.; Macdonald, S. J.; Jamieson, C.; Watson, A. J. Development of Autotaxin Inhibitors: An Overview of the Patent and Primary Literature. *J. Med. Chem.* **2016**, *59* (12), 5604−5621.

(7) Alhouayek, M.; Masquelier, J.; Muccioli, G. G. Lysophosphatidylinositols, from Cell Membrane Constituents to GPR55 Ligands. *Trends Pharmacol. Sci.* **2018**, *39* (6), 586−604.

(8) Yamashita, A.; Oka, S.; Tanikawa, T.; Hayashi, Y.; Nemoto-Sasaki, Y.; Sugiura, T. The Actions and Metabolism of Lysophosphatidylinositol, an Endogenous Agonist for GPR55. *Prostaglandins Other Lipid Mediators* **2013**, *107*, 103−116.

(9) Makide, K.; Uwamizu, A.; Shinjo, Y.; Ishiguro, J.; Okutani, M.; Inoue, A.; Aoki, J. Novel Lysophosphoplipid Receptors: Their Structure and Function. *J. Lipid Res.* **2014**, *55* (10), 1986−1995.

(10) van der Kleij, D.; Latz, E.; Brouwers, J. F.; Kruize, Y. C.; Schmitz, M.; Kurt-Jones, E. A.; Espevik, T.; de Jong, E. C.; Kapsenberg, M. L.; Golenbock, D. T.; Tielens, A. G.; Yazdanbakhsh, M. A Novel Host-Parasite Lipid Cross-Talk. Schistosomal Lyso-Phosphatidylserine Activates Toll-Like Receptor 2 and Affects Immune Polarization. *J. Biol. Chem.* **2002**, *277* (50), 48122−48129.

(11) Ikubo, M.; Inoue, A.; Nakamura, S.; Jung, S.; Sayama, M.; Otani, Y.; Uwamizu, A.; Suzuki, K.; Kishi, T.; Shuto, A.; Ishiguro, J.; Okudaira, M.; Kano, K.; Makide, K.; Aoki, J.; Ohwada, T. Structure-Activity Relationships of Lysophosphatidylserine Analogs as Agonists of G-Protein-Coupled Receptors GPR34, P2Y10, and GPR174. *J. Med. Chem.* **2015**, *58* (10), 4204−4219.

(12) Kotsikorou, E.; Sharir, H.; Shore, D. M.; Hurst, D. P.; Lynch, D. L.; Madrigal, K. E.; Heynen-Genel, S.; Milan, L. B.; Chung, T. D.; Seltzman, H. H.; Bai, Y.; Caron, M. G.; Barak, L. S.; Croatt, M. P.; Abood, M. E.; Reggio, P. H. Identification of the GPR55 Antagonist Binding Site Using a Novel Set of High-Potency GPR55 Selective Ligands. *Biochemistry* **2013**, *52* (52), 9456−9469.

(13) Sayama, M.; Inoue, A.; Nakamura, S.; Jung, S.; Ikubo, M.; Otani, Y.; Uwamizu, A.; Kishi, T.; Makide, K.; Aoki, J.; Hirokawa, T.; Ohwada, T. Probing the Hydrophobic Binding Pocket of G-Protein-Coupled Lysophosphatidylserine Receptor GPR34/LPS1 by Docking-Aided Structure-Activity Analysis. *J. Med. Chem.* **2017**, *60* (14), 6384−6399.

(14) Chen, D. H.; Naydenov, A.; Blankman, J. L.; Mefford, H. C.; Davis, M.; Sul, Y.; Barloon, A. S.; Bonkowski, E.; Wolff, J.; Matsushita, M.; Smith, C.; Cravatt, B. F.; Mackie, K.; Raskind, W. H.; Stella, N.; Bird, T. D. Two Novel Mutations in ABHD12: Expansion of the Mutation Spectrum in PHARC and Assessment of Their Functional Effects. *Hum. Mutat.* **2013**, *34* (12), 1672−1678.

(15) Fiskerstrand, T.; H'Mida-Ben Brahim, D.; Johansson, S.; M'Zahem, A.; Haukanes, B. I.; Drouot, N.; Zimmermann, J.; Cole, A. J.; Vedeler, C.; Bredrup, C.; Assoum, M.; Tazir, M.; Klockgether, T.; Hamri, A.; Steen, V. M.; Boman, H.; Bindoff, L. A.; Koenig, M.; Knappskog, P. M. Mutations in ABHD12 Cause the Neurodegenerative Disease PHARC: An Inborn Error of Endocannabinoid Metabolism. *Am. J. Hum. Genet.* **2010**, *87* (3), 410−417.

(16) Blankman, J. L.; Long, J. Z.; Trauger, S. A.; Siuzdak, G.; Cravatt, B. F. ABHD12 Controls Brain Lysophosphatidylserine Pathways That Are Deregulated in a Murine Model of the Neurodegenerative Disease PHARC. *Proc. Natl. Acad. Sci. U. S. A.* **2013**, *110* (4), 1500−1505.

(17) Wu, C.; Jin, X.; Tsueng, G.; Afrasiabi, C.; Su, A. I. BioGPS: Building Your Own Mash-up of Gene Annotations and Expression Profiles. *Nucleic Acids Res.* **2016**, *44* (D1), D313−316.

(18) Viader, A.; Ogasawara, D.; Joslyn, C. M.; Sanchez-Alavez, M.; Mori, S.; Nguyen, W.; Conti, B.; Cravatt, B. F. A Chemical Proteomic Atlas of Brain Serine Hydrolases Identifies Cell Type-Specific Pathways Regulating Neuroinflammation. *eLife* **2016**, *5*, No. e12345.

(19) Ogasawara, D.; Ichu, T. A.; Vartabedian, V. F.; Benthuysen, J.; Jing, H.; Reed, A.; Ulanovskaya, O. A.; Hulce, J. J.; Roberts, A.; Brown, S.; Rosen, H.; Teijaro, J. R.; Cravatt, B. F. Selective Blockade of the Lyso-PS Lipase ABHD12 Stimulates Immune Responses In Vivo. *Nat. Chem. Biol.* **2018**, *14* (12), 1099−1108.

(20) Cognetta, A. B., 3rd; Niphakis, M. J.; Lee, H. C.; Martini, M. L.; Hulce, J. J.; Cravatt, B. F. Selective N-Hydroxyhydantoin Carbamate Inhibitors of Mammalian Serine Hydrolases. *Chem. Biol.* **2015**, *22* (7), 928−937.

(21) Leung, D.; Hardouin, C.; Boger, D. L.; Cravatt, B. F. Discovering Potent and Selective Reversible Inhibitors of Enzymes in Complex Proteomes. *Nat. Biotechnol.* **2003**, *21* (6), 687−691.

(22) Liu, Y.; Patricelli, M. P.; Cravatt, B. F. Activity-Based Protein Profiling: the Serine Hydrolases. *Proc. Natl. Acad. Sci. U. S. A.* **1999**, *96* (26), 14694−14699.

(23) Patricelli, M. P.; Giang, D. K.; Stamp, L. M.; Burbaum, J. J. Direct Visualization of Serine Hydrolase Activities in Complex Proteomes Using Fluorescent Active Site-Directed Probes. *Proteomics* **2001**, *1* (9), 1067−1071.

(24) Speers, A. E.; Adam, G. C.; Cravatt, B. F. Activity-Based Protein Profiling In Vivo Using a Copper(i)-Catalyzed Azide-Alkyne [3 + 2] Cycloaddition. *J. Am. Chem. Soc.* **2003**, *125* (16), 4686−4687.

(25) Rostovtsev, V. V.; Green, L. G.; Fokin, V. V.; Sharpless, K. B. A Stepwise Huisgen Cycloaddition Process: Copper(I)-Catalyzed Regioselective "Ligation" of Azides and Terminal Alkynes. *Angew. Chem., Int. Ed.* **2002**, *41* (14), 2596−2599.

(26) Onderwater, R. C.; Commandeur, J. N.; Menge, W. M.; Vermeulen, N. P. Activation of Microsomal Glutathione S-Transferase and Inhibition of Cytochrome P450 1A1 Activity as a Model System for

DOI: 10.1021/acs.jmedchem.8b01958
J. Med. Chem. XXXX, XXX, XXX−XXX

Detecting Protein Alkylation by Thiourea-Containing Compounds in Rat Liver Microsomes. *Chem. Res. Toxicol.* **1999**, *12* (5), 396−402.
(27) Aoki, J.; Nagai, Y.; Hosono, H.; Inoue, K.; Arai, H. Structure and Function of Phosphatidylserine-Specific Phospholipase A1. *Biochim. Biophys. Acta, Mol. Cell Biol. Lipids* **2002**, *1582* (1−3), 26−32.
(28) Kamat, S. S.; Camara, K.; Parsons, W. H.; Chen, D. H.; Dix, M. M.; Bird, T. D.; Howell, A. R.; Cravatt, B. F. Immunomodulatory Lysophosphatidylserines Are Regulated by ABHD16A and ABHD12 Interplay. *Nat. Chem. Biol.* **2015**, *11* (2), 164−171.
(29) Inloes, J. M.; Jing, H.; Cravatt, B. F. The Spastic Paraplegia-Associated Phospholipase DDHD1 Is a Primary Brain Phosphatidylinositol Lipase. *Biochemistry* **2018**, *57* (39), 5759−5767.
(30) Daigneault, M.; Preston, J. A.; Marriott, H. M.; Whyte, M. K.; Dockrell, D. H. The Identification of Markers of Macrophage Differentiation in PMA-Stimulated THP-1 Cells and Monocyte-Derived Macrophages. *PLoS One* **2010**, *5* (1), No. e8668.
(31) Schwende, H.; Fitzke, E.; Ambs, P.; Dieter, P. Differences in the State of Differentiation of THP-1 Cells Induced by Phorbol Ester and 1,25-Dihydroxyvitamin D3. *J. Leukocyte Biol.* **1996**, *59* (4), 555−561.
(32) Tsuchiya, S.; Kobayashi, Y.; Goto, Y.; Okumura, H.; Nakae, S.; Konno, T.; Tada, K. Induction of Maturation in Cultured Human Monocytic Leukemia Cells by a Phorbol Diester. *Cancer Res.* **1982**, *42* (4), 1530−1536.
(33) Lichtman, A. H.; Leung, D.; Shelton, C. C.; Saghatelian, A.; Hardouin, C.; Boger, D. L.; Cravatt, B. F. Reversible Inhibitors of Fatty Acid Amide Hydrolase That Promote Analgesia: Evidence for an Unprecedented Combination of Potency and Selectivity. *J. Pharmacol. Exp. Ther.* **2004**, *311* (2), 441−448.

DOI: 10.1021/acs.jmedchem.8b01958
J. Med. Chem. XXXX, XXX, XXX−XXX